

# UC Irvine

## UC Irvine Electronic Theses and Dissertations

### Title

Silver-Indium Solid Solution on Copper as Passivation and Study of its Reaction with Tin Solder

### Permalink

<https://escholarship.org/uc/item/5s17x5d9>

### Author

Wu, Yipin

### Publication Date

2018

Peer reviewed|Thesis/dissertation

UNIVERSITY OF CALIFORNIA,  
IRVINE

Silver-Indium Solid Solution on Copper as Passivation  
and Study of its Reactions with Tin Solder

THESIS

submitted in partial satisfaction of the requirements  
for the degree of

MASTER OF SCIENCE

in ENGINEERING

by

Yipin Wu

Thesis Committee:  
Professor Chin C. Lee, Chair  
Professor Frank Shi  
Professor James Earthman

2018



## TABLE OF CONTENTS

	Page
<b>LIST OF FIGURES</b>	iii
<b>LIST OF TABLES</b>	v
<b>ACKNOWLEDGMENTS</b>	vi
<b>ABSTRACT OF THE THESIS</b>	vii
<b>1. INTRODUCTION</b>	1
<b>2. EXPERIMENTAL SETUP AND CHARACTERIZATION TECHNIQUES</b>	4
2.1 Scanning Electron Microscopy/Energy Dispersive X-Ray Spectroscopy	4
2.2 X-Ray Diffraction	5
2.3 E-beam Evaporation	6
2.4 Electroplating Process	7
<b>3. REACTION STUDY OF SN ON (AG)9.5IN DISKS</b>	8
3.1 Experimental Design	8
3.2 Results and Discussion	9
<b>4. (AG)9.5IN COATINGS ON CU SUBSTRATES AS PROTECTION LAYER AND TIN</b>	17
<b>SOLDERING REACTION STUDY</b>	
4.1 (Ag)9.5In on Cu Aging Study	17
4.2 Tin Soldering Reaction Study	20
4.2.1 Experimental Setup	20
4.2.2 Results and Discussion	22
<b>5. SUMMARY AND CONCLUSIONS</b>	30
<b>REFERENCES</b>	31

## LIST OF FIGURES

		Page
Figure 1.1	A schematic diagram of a solder joint between leg of copper leadframe and substrate board.	2
Figure 2.1	Signals emitted from different parts of the interaction volume in SEM	5
Figure 2.2	A schematic diagram of e-beam evaporation process and evaporator setup.	6
Figure 3.1	Experimental design of reaction of (Ag)In disk with Sn.	9
Figure 3.2	Cross-section of Ag/Sn and (Ag)In/Sn reaction optical microscope.	9
Figure 3.3	Cross-section of Ag/Sn and (Ag)In/Sn reaction after etching under optical microscope.	10
Figure 3.4	Cross-section of Ag/Sn and (Ag)In/Sn reaction after etching under SEM (backscattering imaging).	12
Figure 3.5	Point analysis position on disk (Ag)In/Sn sample for EDX.	13
Figure 3.6	XRD pattern with peak identifications for Ag/Sn and (Ag)In/Sn samples.	16
Figure 4.1	A photo of the surface finish comparison of as (Ag)In coated, 143hr aging, 1000hr aging and bare copper 1000hr aging samples.	17
Figure 4.2	SEM image of the surface of (a) (Ag)In coated 1000hr aging, (b) bare Cu 1000hr aging.	18

Figure 4.3	Cross-section image of (Ag)In coated samples (a) As deposited, (b) 148hr aging.	19
Figure 4.4	A photo of the experimental setup. Since tin melts in the process, the temperature is monitored by the center thermal couple on a bare copper substrate instead of the actual sample.	21
Figure 4.5	Temperature profile of the reflow process in the vacuum bonder.	22
Figure 4.6	As-reflowed Sn soldering reaction samples with (Ag)In coated Cu substrate on the left side and bare Cu substrate on the right side.	23
Figure 4.7.	Surface of Sn on (Ag)In Coated Cu and Sn on Bare Cu samples after different hours of aging at 175°C.	24
Figure 4.8	Cross-section SEM (BSE mode) image of as reflowed samples of (a) Sn on (Ag)In coated Cu, (b) Sn on bare Cu.	25
Figure 4.9	EDX mapping of as reflowed Sn on (Ag)In coated Cu sample.	26
Figure 4.10	Cross-section SEM (BSE) image of Sn on (Ag)In coated Cu and Sn on bare Cu samples aged at 175°C for different hours.	27
Figure 4.11	Plot of $Cu_6Sn_5$ and $Cu_3Sn$ IMC thicknesses (both separated and combined) of (Ag)In coated and bare Cu samples at different aging time.	28
Figure 4.12	An illustration of IMC growth of the reaction between (Ag)In coated Cu and Sn.	29

## LIST OF TABLES

		Page
Table 3.1	EDX point analysis results for disk (Ag)In/Sn sample	14
Table 3.2	Lattice constant calculated from XRD pattern for Ag/Sn and (Ag)In/Sn.	16

## ACKNOWLEDGMENTS

I would like to express my deepest appreciation to my committee chair and mentor Dr. Chin. C. Lee for his kind advices and giving me the chance to explore the world of electronics packaging. Without his guidance, this thesis can't be finished. I would like to acknowledge my committee members, Dr. Frank Shi and Dr. James Earthman, for providing me advice and supervising the thesis. I would also thank my fellow labmates, Dr. Yongjun Huo, PhD candidate Jiaqi Wu and Shao-Wei Fu, for teaching me the basics, training me the instruments, and providing me suggestions and ideas when I lost my directions.

I would like to thank all my friends that have been supporting me and cheering me up. I want to especially thank my friend Michael Liao. His passion for chemistry, materials science and music shows me the importance of persisting in pursuing one's own dream. He motivates me to keep having curiosity of knowledge and never give up on my dream.

Lastly, I want to say thank you to my family. My grandmother, my parents and my sister have always been my strongest support. Thanks for encouraging me to choose what I want to do and teaching me to stay positive regardless of the obstacles I face.

To my grandfather in heaven, I miss you and I love you.



## **ABSTRACT OF THE THESIS**

Silver-Indium Solid Solution on Copper as Passivation  
and Study of its Reactions with Tin Solder

By

Yipin Wu

Master of Science in Engineering, Materials and Manufacturing Technology

University of California, Irvine, 2018

Professor Chin C. Lee, Chair

As the most commonly used electrode, leadframe, and package material in electronic packaging, copper (Cu) has severe oxidation problem, preventing wetting during soldering processes and prohibiting successful wire bonding. Thus leads and bond pads of leadframes and packages are often coated with a passivation layers such as palladium, silver, or tin, which suppresses the growth of copper oxides. In this research, I investigated the use of silver-indium ((Ag)In) solid solution as a new alternative coating material for passivation. First, a reaction study of bulk (Ag)-9.5In solid solution disks with Sn was conducted to evaluate possible intermetallic compounds in the Ag-In-Sn system. Next, (Ag)-9.5In solid solution layer was coated on copper substrates by E-beam evaporation. The (Ag)9.5In-passivated Cu substrates and bare Cu substrates were aged at 150°C for up to 1000 hours in air. No oxide was detectable on (Ag)9.5In-passivated Cu substrates while thick  $\text{Cu}_2\text{O}_3$  was grown on bare Cu. This result illustrates that (Ag)9.5In solid solution is an excellent passivation coating material. Then, (Ag)9.5In-passivated Cu substrates were electroplated with tin. As a reference, bare Cu substrates were also plated with tin. These two different types of samples were reflowed and aged for different amount of time. No flux

was used. The reaction results were examined by scanning electron microscope/energy dispersive X-ray spectroscopy (SEM/EDX) and compared. The experimental results show that tin wetted and reacted well with (Ag)9.5In-passivated Cu substrates. The growth of intermetallic compound ( $\text{Cu}_6\text{Sn}_5$ ,  $\text{Cu}_3\text{Sn}$ ) on (Ag)9.5In-passivated Cu substrates is also suppressed compared to the growth on bare Cu substrates. The design of (Ag)In solid solution passivation is an invention and its superior performance is a discovery. It provides an economical, environmentally friendly, and valuable passivation alternative on copper electrodes, leadframes, and packages.

## 1. INTRODUCTION

In electronic packaging, copper (Cu) has been widely used as electrode, package, and leadframe material. In the leadframe application, the circuits of Si chip is connected to Cu leadframe by wire bonding, and the leadframe legs are joined to bond pads on a printed circuit board (PCB) by solder [1]. A schematic diagram of the structure is shown in Figure 1.1. Copper by nature is readily to be oxidized when exposed to air and the oxidation is severer at high temperature. Copper oxide layer drastically decreases the solderability. A common way to prevent copper oxidation is by plating a layer of tin (Sn) as leadframe finish. However, tin plating can cause the growth of Sn whiskers. Whisker growth is a stress relief phenomenon driven by the compressive stress due to the room temperature reaction between Cu and Sn [2]. Sn whiskers can grow several hundred microns, which are long enough to connect neighboring legs on the leadframe and short the circuits. In 1991, Abbott et al [3] from Texas Instruments proposed to use palladium as a lead finish for surface mount IC packages. They claimed that with palladium layer, no intermetallic layers could form while having good solderability and reliability. However, palladium is a very costly material, which significantly raises the cost of product.

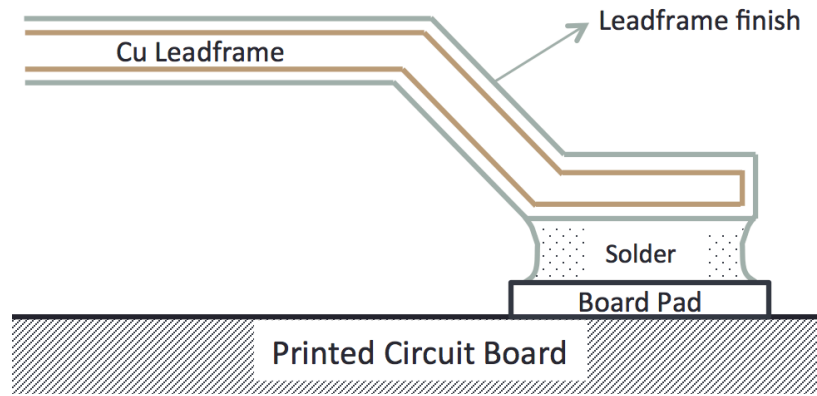


Figure 1.1. A schematic diagram of a solder joint between leg of copper leadframe and substrate board.

Silver indium ((Ag)In) solid solution has many superior properties, both chemically and mechanically, that discovered by our group. Silver has a very serious problem that any sulfur in air can tarnish the surface to form silver sulfide. This disadvantage can cause a lot of reliability issues when using silver in the electronic packaging. Previously, it has been found that adding indium to silver, making it a solid solution, can have good anti-tarnishing property, and it has been examined through a designed sulfur vapor test method [4]. Additionally, (Ag)In solid solution also exhibits great mechanical property and oxidation resistance. These preferred properties makes (Ag)In a potential coating material for Cu leadframe, preventing Cu from severe oxidation and extending its shelf life.

Besides examining the feasibility of using (Ag)In as an anti-oxidation layer, soldering reaction is another factor needs to take into consideration. After coating, the leadframe needs to maintain its solderability in order to have good interconnections. Intermetallic compound (IMC) growth is a sign of bonding and good connection between two materials. However, a thick layer of IMC may weaken the joints since most of IMC are very brittle. Many studies were done on exploring the relationship between IMC growth

and the solder joint strength. It is certain that the growth of intermetallic compounds formed in the solder joint can cause long-term reliability issues [5] [6].

This preliminary study uses pure tin as solder in the experiments because the use lead-tin (Pb-Sn) solder in electronics industry is prohibited by Restriction of Hazardous Substances directive (RoHS) in European which implemented in 2006 to reduce toxic electronic wastes. With the environmental concern, the United States also encourages the manufacturers to reduce lead-based solders. Thus, industries gradually replaced lead-based solders to lead-free solders, which most of those nowadays are high-Sn based, for example, SAC305 contains 96.5% Sn, 3% Ag, and 0.5% Cu. To study the soldering reaction by using Sn will give us a good idea of how the (Ag)In coated on Cu perform with other high-Sn based solders.

The reaction of bulk (Ag)In solid solution disk with Sn is firstly studied in order to examine the possible intermetallic compounds growth in (Ag)In-Sn system. Secondly, an aging study of (Ag)In coated Cu substrate is conducted to examine the oxide growth on the (Ag)In coated surface. Lastly, soldering reaction of (Ag)In coated Cu with Sn is examined and compared at different aging time after reflow.

## **2. EXPERIMENTAL SETUP AND CHARACTERIZATION TECHNIQUES**

### **2.1 Scanning Electron Microscopy/Energy Dispersive X-Ray Spectroscopy**

Scanning Electron Microscope is a tool to observe specimen surfaces by using focused electron beam. When the specimen irradiates with the focused electron beam, several different signals are emitted. These signals include secondary electron (SE), backscattered electron (BSE), characteristic X-rays, cathodoluminescence, etc. SEM utilizes these signals to observe and analyze the specimen surface. Because the energy of secondary electrons is small, and those generated in a deep region are quickly absorbed by the specimen, only the signals generated at the top surface can be emitted and detected by the SE detector installed in SEM. Thus, secondary electron, which is sensitive to the surface, can be used to observe the morphology and topography of the specimen surface.

Backscattered electrons are the electrons scattered backward and emitted out of the specimen when there is incident electron beam. Backscattered electrons are sensitive to the composition of the specimen because the backscattered electron intensity increases as atomic number  $Z$  increases. In SEM, BSE detector is able to collect backscattered electron signals. BSE image contains information of composition of the specimen: the specimen region with heavier elements appears lighter in BSE image [8].

Energy dispersive X-ray spectrometer (EDX) can also be installed in SEM, and is used to analyze characteristic X-ray spectra. The detector receives the X-ray emitted from the specimen and produces an X-ray spectrum. Different X-ray energy peaks in the X-ray spectrum correspond to different elements. By using supplementary EDX software, quantitative analysis in a small area (point analysis) as well as EDX mapping can be conducted. Thus, energy dispersive X-ray spectroscopy can be used to determine the

element composition of the specimen in certain area. In this study, Philips XL-30 FEG SEM was used to examine the cross-sections of the samples.

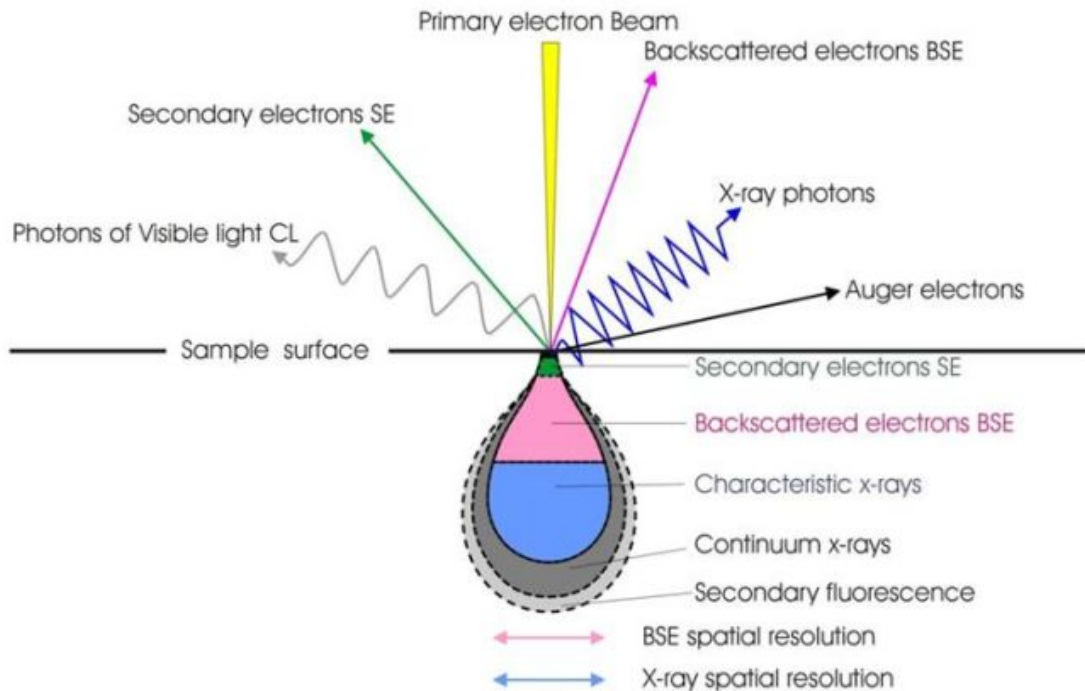


Figure 2.1. Signals emitted from different parts of the interaction volume in SEM [9].

## 2.2 X-Ray Diffraction

X-ray diffraction is a non-destructive analytical technique to determine the chemical composition and molecular structure of a crystal. It can be used for identification of crystalline phases of various materials. X-ray is generated by cathode ray tube, and filtered to be monochromatic. The constructive interference occurs when it satisfies Bragg's law, shown in equation (1),

$$n\lambda = 2d \sin \theta \quad (1)$$

where  $n$  is an integer,  $\lambda$  is the wavelength of x-ray,  $d$  is the lattice spacing of the crystalline sample, and  $\theta$  is the diffraction angle. Diffracted intensities and corresponding angles are

determined by the atomic arrangement of the lattice planes. Thus, with the XRD pattern detected, one can identify the crystal structure, lattice constant, and other characteristics of the specimen [10]. In this study, Rigaku Smart Lab X-ray Diffractometer is used to perform XRD analysis.

### 2.3 E-beam Evaporation

E-beam evaporation is a form of physical vapor deposition in which a target material is bombarded with electron beam from a charged tungsten filament to evaporate target material for deposition coating on substrate. A schematic diagram is shown in figure 2.2. Electron beam evaporation has many advantages over resistive thermal evaporation. It can yield high deposition rates, from 0.1nm per minute to 100nm per minute. Another advantage is that because e-beam only melts target material but not the crucible, contamination from neighboring components can be eliminated, yields high purity thin film deposition [11].

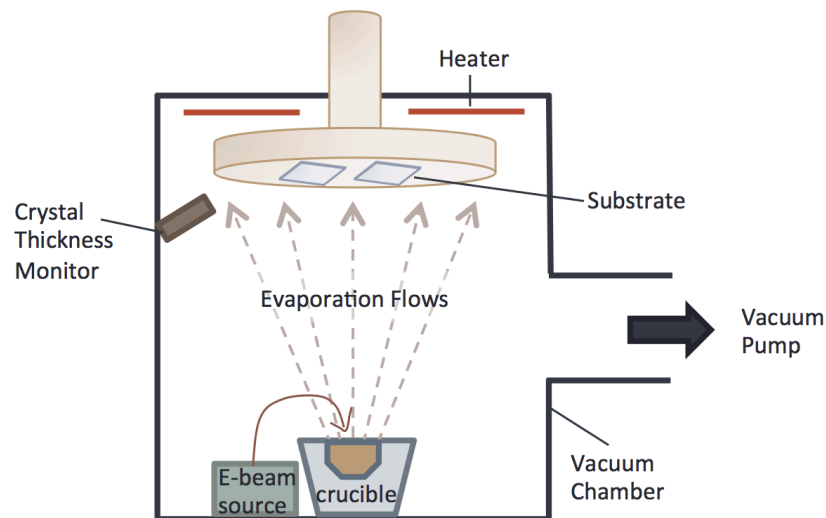


Figure 2.2. A schematic diagram of e-beam evaporation process and evaporator setup.



E-beam evaporation also enables the possibility of depositing solid solution with a certain composition onto a substrate. Because the melting point and partial pressure of silver and indium are different, silver and indium shots in the crucible needs to be tuned in order to deposit desired composition. In this study, Ångstrom E-beam Evaporator was used to deposit (Ag)-9.5In thin film on copper substrate with a specific composition recipe.

## **2.4 Electroplating Process**

Electroplating is a process of depositing one metal onto another metal by electrical current. The electroplating process involves a cathode, an anode and electrolyte solution. Two electrodes connecting to power source immersed in electrolyte solution with desired metal. Plating material is used as anode and substrate of plating is used at cathode. When power is supplied, the metal atoms oxidize to ions at the anode side and dissolve in the solution. The dissolved ions are reduced at the cathode side which forms a plating layer on the cathode. Electroplating is used massively in industry for various purposes. In this study, electroplating method is used to deposit Sn on the substrates.

### 3. REACTION STUDY OF SN ON (AG)9.5IN DISKS

#### 3.1 Experimental Design

To study the bulk reaction of (Ag)In solid solution with Sn, (Ag)In disks with several millimeters thick are used as the substrates and Ag disks are used as a reference. Both Ag and (Ag)-9.5In disk were cut from (Ag)-9.5In ingot grown by our group by using diamond saw. The surface was polished by silicon carbide paper and diamond suspension to 3 $\mu$ m. The disks were then electroplated with Sn. The backside of the disk was taped so that the Sn will only plate on one side of the disk. The thickness of the electroplated layer is related to the time of electroplating, and theoretically can be calculated by (2a) and (2b)

$$mass\ deposited = \frac{I \cdot t \cdot MM}{F \cdot n} \quad (2a)$$

$$thickness = \frac{mass\ deposited}{\rho \cdot area} = \frac{I \cdot t \cdot MM}{F \cdot n \cdot \rho \cdot area} \quad (2b)$$

where I is the current, t is the time in seconds, MM is the molar mass, F is the Faraday's constant, n is the number of electron transfer,  $\rho$  is the density of the element. The substrates were electroplated for 60 min. After electroplating, the samples were reflowed in a convectional oven with a peak temperature of 250 $^{\circ}$ C for 1 min, which was monitored by a thermal couple. After reflowing, the samples were cooled at the room temperature. The samples were mounted by using epoxy and cut into half by diamond saw. The cross-section was polished and examined by optical microscope (OM) as well as the SEM/EDX to determine the existing phases. XRD was also used to characterize the IMC phase grown after the reflow.

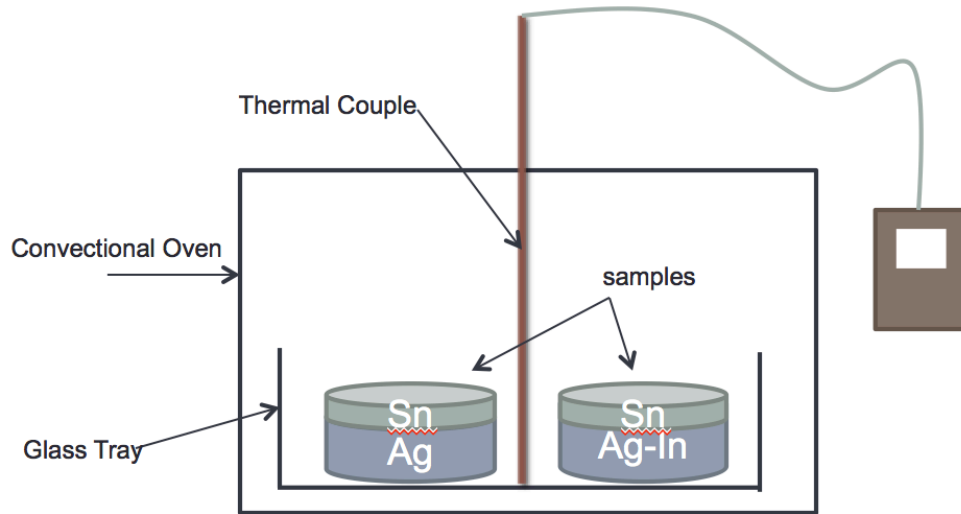


Figure 3.1. Experimental design of reaction of (Ag)In disk with Sn.

### 3.2 Result and Discussion

The cross-section of the samples has been examined first by optical microscope (OM) and shown in figure 3.2. The IMC layer is around  $10\mu\text{m}$  thick with a deeper color under OM. No obvious difference between Ag/Sn and (Ag)In/Sn reaction can be observed in OM images.

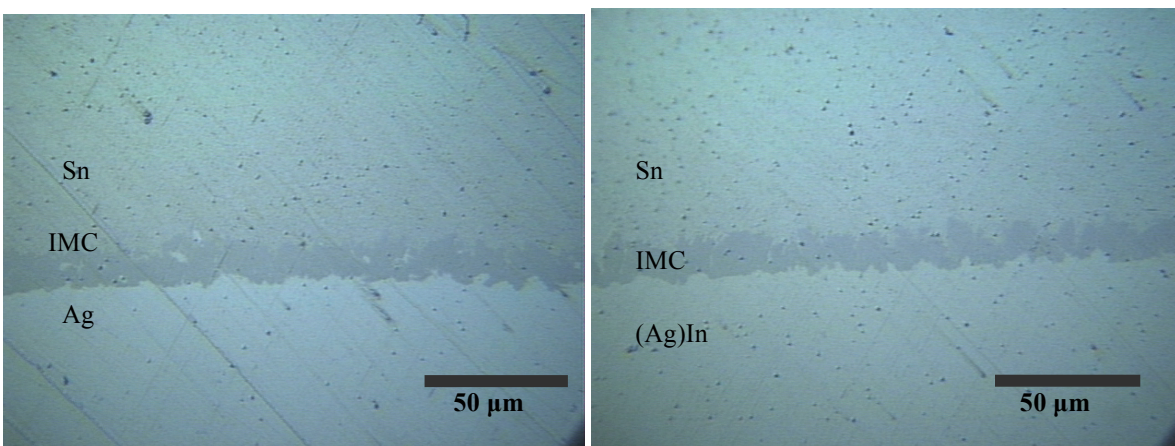


Figure 3.2. Cross-section of Ag/Sn and (Ag)In/Sn reaction under optical microscope.

In order to identify the IMC layer and examine the phases under a higher magnification, the samples need to be examined by SEM as well. To ensure the IMC layer will also be distinguishable under SEM, the surface of the cross-section is treated by 1.2M hydrochloric acid (HCl) solution. Since HCl solution can only etch away Sn layer but not the IMC and Ag layer, the morphology of the IMC layer can be shown clearly later under the SEM. The samples after etching are shown in figure 3.3. The samples are then sputter coated with a thin layer of Au/Pd to make the surface conductive in order to conduct SEM/EDX characterization.

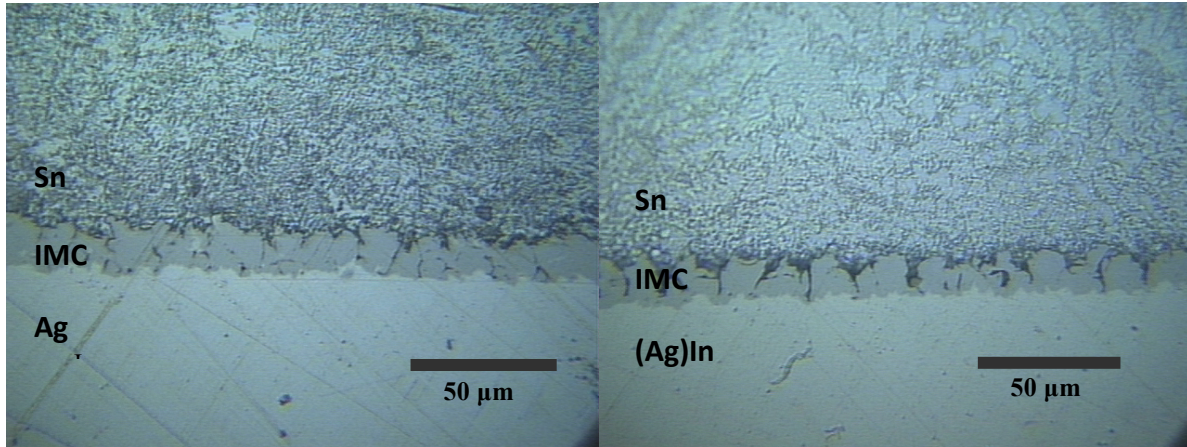


Figure 3.3. Cross-section of Ag/Sn and (Ag)In/Sn reaction after etching under optical microscope.

Figure 3.4 shows the images taken under SEM backscattering mode. Similar as under optical microscope, the cross-section has three layers: Sn, IMC, and Ag or (Ag)In. Sn layer and IMC layer has morphology contrast due to the etching; IMC layer and Ag or (Ag)In layer has a color contrast due to the composition difference. The thickness of the IMC layer in both Sn/Ag and Sn/(Ag)In is about the same.

Su et al. [10] have been studied the reaction between liquid Sn and Ag substrate. The only intermetallic compound grown in such reaction is  $\text{Ag}_3\text{Sn}$ . In results of soldering reaction between Sn and Ag substrate, scallop-shaped  $\text{Ag}_3\text{Sn}$  appears at Ag/Sn interface and needle-shaped  $\text{Ag}_3\text{Sn}$  precipitates was observed in the Sn matrix due to the dissolution of Ag into the liquid Sn matrix. In this study, the Ag/Sn sample has similar observation as Su et al., and the composition of IMC phase has been confirmed by EDX. EDX shows the IMC composition to be  $\text{Ag}_3\text{Sn}$ , with around 74.5 at.% Ag and 25.5 at.% Sn.

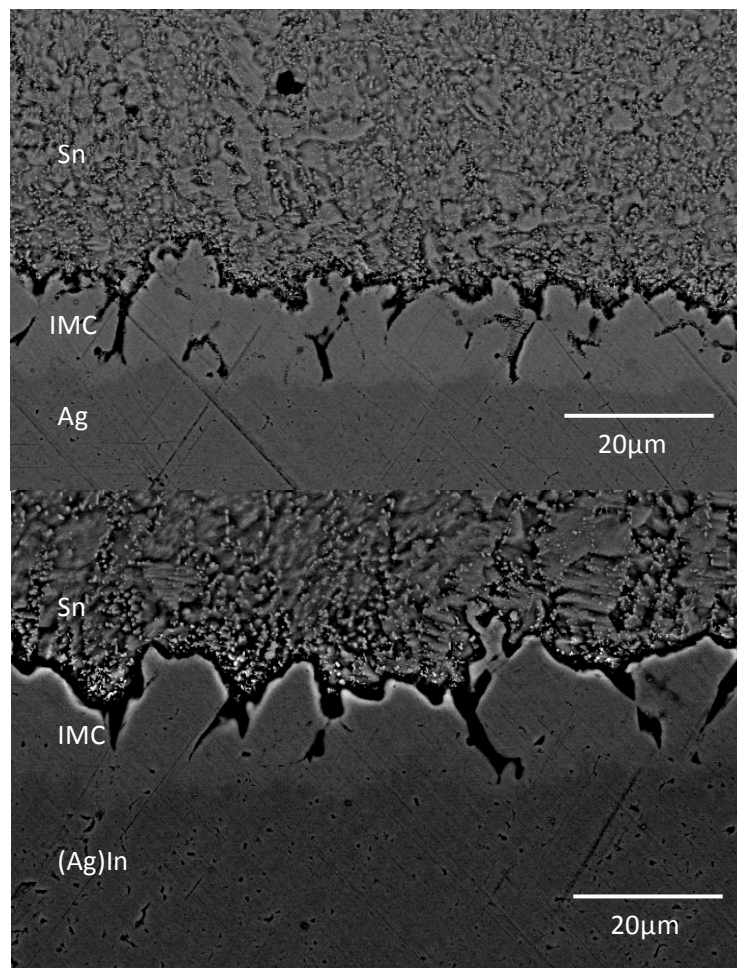


Figure 3.4. Cross-section of Ag/Sn and (Ag)In/Sn reaction after etching under SEM (backscattering imaging).

(Ag)In/Sn sample has also been examined by EDX and the results are shown in Figure 3.5 and Table 3.1. From the EDX results, the IMC phase also appears to be  $\text{Ag}_3\text{Sn}$ . One thing to notice is that on the (Ag)In disk side, around 9.5 at.% In can be detected by EDX, however, no indium can be detected anywhere in the IMC phase as well as the Sn matrix. At first, the assumption is that instead of reacting or migrating towards the Sn matrix, indium tends to stay at the (Ag)In phase. If that is the case, a higher indium concentration should be detected near (Ag)In and IMC interface. However, EDX point analysis of the (Ag)In phase shows a relatively uniform composition of the original (Ag)In solid solution in vertical direction, which means there's no evidence of indium accumulation at (Ag)In phase.

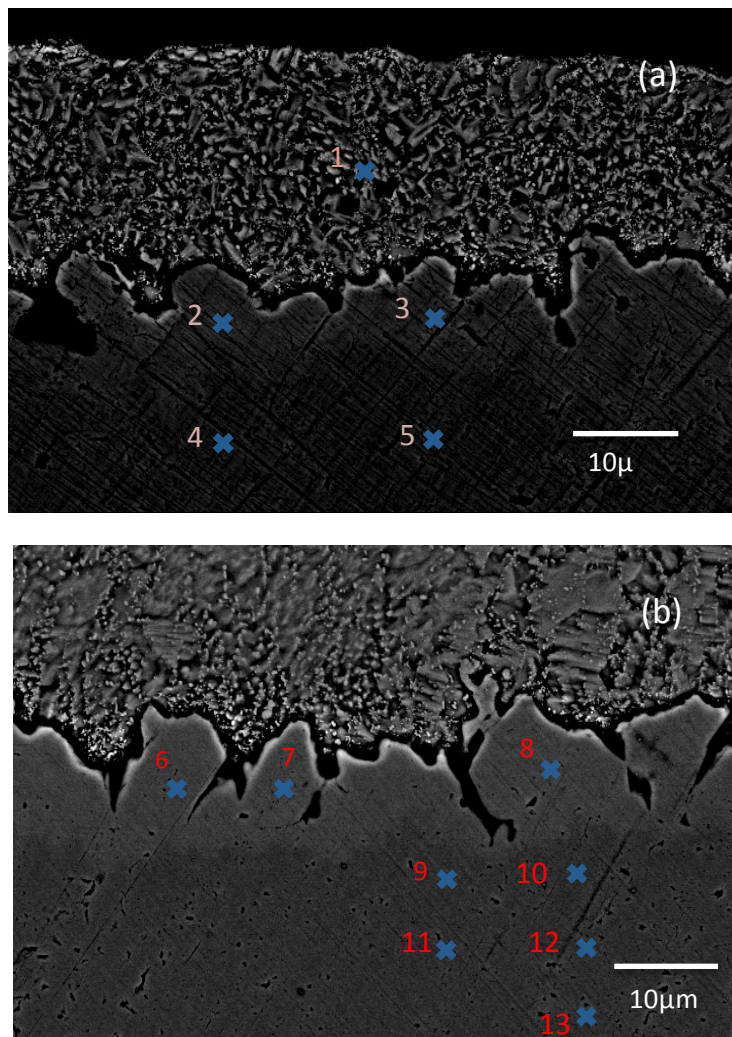


Figure 3.5. Point analysis position on disk (Ag)In/Sn samples for EDX.

(a)

Point	Ag	In	Sn
1	2.1		97.9
2	75.1		24.9
3	74.5		25.5
4	91.0	9.0	

<b>5</b>	91.1	8.9	
----------	------	-----	--

(b)

<b>Point</b>	<b>Ag</b>	<b>In</b>	<b>Sn</b>
<b>6</b>	74.2		25.8
<b>7</b>	73.7		26.3
<b>8</b>	73.7		26.3
<b>9</b>	90.6	9.4	
<b>10</b>	90.6	9.4	
<b>11</b>	90.9	9.1	
<b>12</b>	90.5	9.5	
<b>13</b>	90.4	9.6	

Table 3.1. EDX point analysis results for disk (Ag)In/Sn samples

Back to the basics of EDX, the detector receives the characteristic X-ray signals and elements are determined by differentiating the energy level. In case of indium and tin, the characteristic X-ray energy levels are very close to each other. As a result, indium signals didn't differentiated from the tin signals by the auto peak identification, especially when indium amount is low.

X-ray diffraction is also performed on the surface of the sample to examine the possible IMC phase in the system. To obtain sufficient penetration, surface tin layer is etched by using diluted HCl so that IMC phase can have a better exposure to the X-ray. The XRD results are shown in Figure 3.6. Major peaks for both Ag/Sn and (Ag)In/Sn samples are from Sn and Ag<sub>3</sub>Sn; a small amount of Ag signal from the Ag disk is detected in Ag/Sn



sample. No additional peaks from other IMC can be observed in the (Ag)In/Sn sample, indicating no indium related IMCs grown in the reaction. The lattice constants of both samples calculated from XRD pattern are shown in Table 3.2. Sn lattice constants in two spectra differ by around 0.0001 while  $\text{Ag}_3\text{Sn}$  lattice constants differ by around 0.01. In Ag-In-Sn phase diagram study, some group indicated that the  $\text{Ag}_3\text{Sn}$  can dissolve up to 2 at.% In [12]. The lattice constant difference of  $\text{Ag}_3\text{Sn}$  may be an indication of indium atoms may partially dissolved in  $\text{Ag}_3\text{Sn}$ .

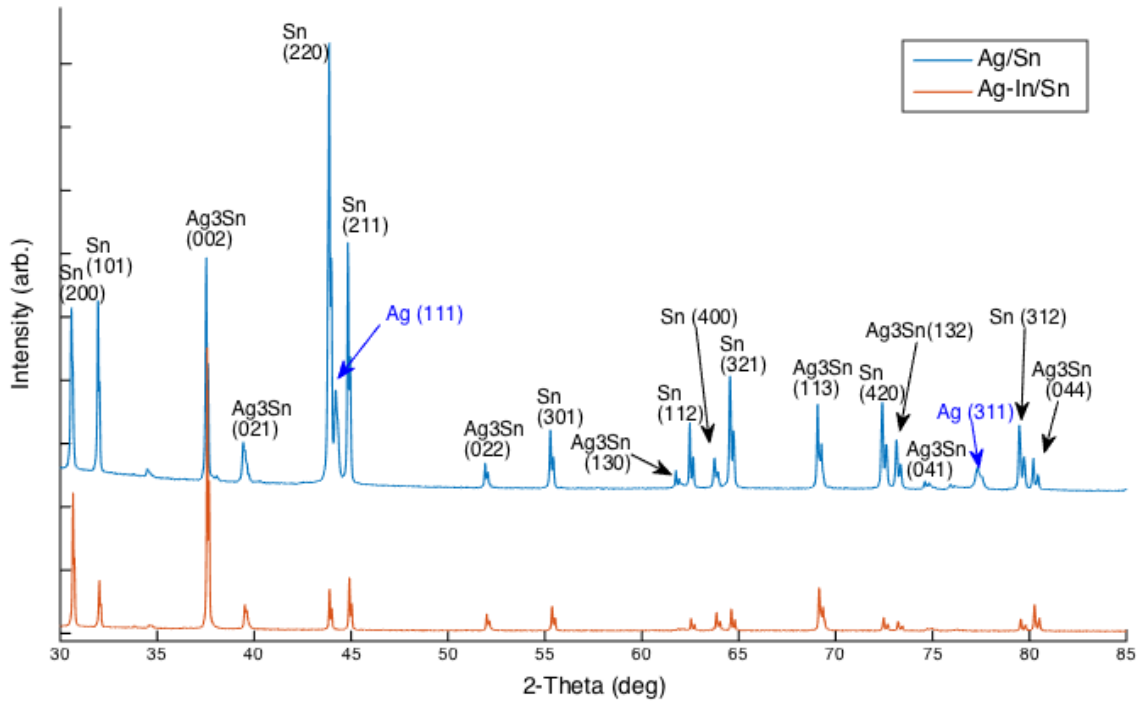


Figure 3.6. XRD pattern with peak identifications for Ag/Sn and (Ag)In/Sn samples. Peaks written in black stands for peaks appear in both Ag/Sn and (Ag)In/Sn sample. Peaks written in blue stands for peaks only appear in Ag/Sn sample.

Phase	a (Å)	b (Å)	c (Å)
Sn (Ag/Sn)	5.827928	5.827928	3.180459
Ag <sub>3</sub> Sn (Ag/Sn)	5.985422	4.778890	5.186698
Sn ((Ag)In/Sn)	5.828597	5.828597	3.180068
Ag <sub>3</sub> Sn ((Ag)In/Sn)	5.993255	4.781584	5.173750

Table 3.2. Lattice constant calculated from XRD pattern for Ag/Sn and (Ag)In/Sn.

## 4. (AG)IN COATINGS ON CU SUBSTRATES AS PROTECTION LAYER AND TIN SOLDERING REACTION STUDY

### 4.1 (Ag)In on Cu Aging Study

Copper substrates were protected by polymer film before use. After peeling off the polymer film, substrates were firstly immersed in acetone and sonicated for 2 min to remove organic residue, then the substrates were immersed in diluted HCl to remove copper oxides. In the first run of e-beam evaporation, 500nm of (Ag)5In was then coated on Cu substrate. Three samples were aged in a convection oven at 150°C for 143hr, 454hr, and 1000hr to examine the oxidation at sample surface. A picture of surface finishes of selected samples is shown in Figure 4.1. (Ag)5In coated sample has a silvery, reflective finish, and it can persist its shiny finish under room temperature storage. After aging at 150°C, the surface is still reflective, but become a little bit yellowish as aging time increases. The bare copper substrate, on the other hand, appears dark and tarnished, indicating the severe oxidation occurred at surface.



Figure 4.1. A photo of the surface finish comparison of as (Ag)5In coated, 143hr aging, 1000hr aging and bare copper 1000hr aging samples.

To have a closer look into the surface, the samples are observed under SEM. The top surface SEM images are shown in Figure 4.2. The (Ag)In coated Cu samples show some round-shaped oxide on the surface whereas the bare Cu surface was covered entirely by oxides. The SEM images show that after 1000hr aging at 150°C, (Ag)In coated copper has significantly less oxide compare to the bare copper substrate. Another thing that take into consideration is how (Ag)In coating layer reacts with Cu substrate during aging. Since (Ag)In layer is only 500nm thick, which makes the samples hard to polish mechanically, Focused Ion Beam (FIB) were used to create damage free cross-sections. The cross-section of the (Ag)In coated sample are also observed by SEM and shown in Figure 4.3. The cross-section images show that no visible IMC growth between (Ag)In and Cu after aging. Ag and Cu won't form IMC according to the phase diagram, and In in this situation remains its solid solution form instead of forming Ag-In IMC or Cu-In IMCs.

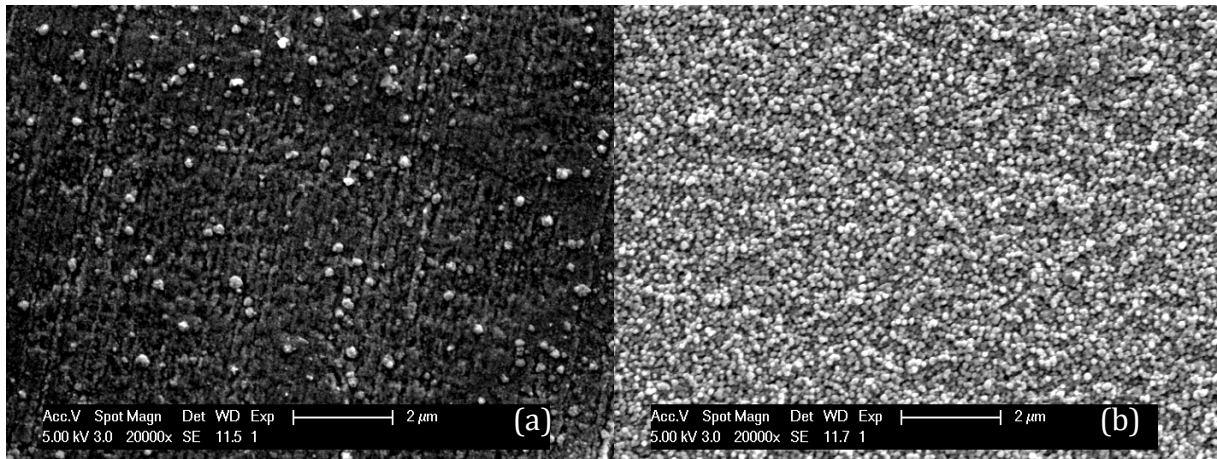


Figure 4.2. SEM image of the surface of (a) (Ag)In coated 1000hr aging, (b) bare Cu 1000hr aging.

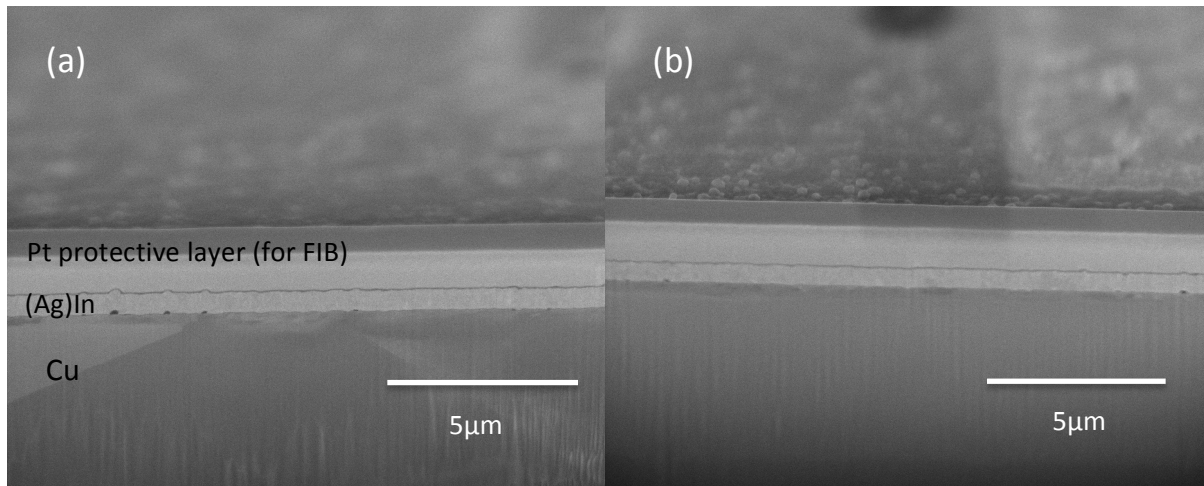


Figure 4.3. Cross-section image of (Ag)In coated samples (a) As deposited, (b) 148hr aging.

## 4.2 Tin Soldering Reaction Study

### 4.2.1 Experimental Setup

After validating its anti-oxidation property, the solderability also needs to be verified. In this experiment, the e-beam deposition recipe was modified and 500nm of (Ag)<sub>9.5</sub>In is deposited on Cu substrate. The (Ag)<sub>9.5</sub>In coated Cu substrates are electroplated with a layer of Sn. According to equation 2a and 2b, the theoretical thickness should be 40 $\mu$ m with 25 min electroplating process. The experimental process has been modified through the study. In the previous (Ag)In-Sn reaction study, it has been found that the temperature control is hard by using a convectional furnace. The initial condition of the furnace is crucial to the reaction, because the temperature reading on the furnace is the ambient air temperature in the furnace whereas the dominating heat transfer process for the samples is conduction from the bottom of the furnace. Due to the furnace setup, supplementary thermal couple can't make contact with the reference sample substrate stably and monitor the substrate temperature; additionally, the reflow reaction can't be seen unless the sample has taken out from the furnace, making the actual reflow time hard to determine. To have a better control with the reflow process, a vacuum bonder is used as reflow oven instead of the convectional furnace. The vacuum bonder designed by our group uses nickel chromium alloy as heating coil, where the substrate temperature can be controlled by the input voltage and monitored by a thermal couple; the experimental setup is shown in Figure 4.4. The advantage is to create a vacuum reflow process with a more precise temperature control and the reflow process is visible; the disadvantage is sample cooling is relatively long. The temperature profile has been created and adjusted as shown in Figure 4.5. The peak temperature is designed to be 250°C and stayed there for about 1

min. Since Sn melts at 231°C, the actual reflow reaction, where temperature is higher than 231°C, is around 9 min. The temperature profile only recorded the time which samples cooled to 120°C, but the time taken for samples cooling to room temperature is approximately 1-2 hr. Three sets of samples were then aged at 175°C in a convectional furnace for different hours.



Figure 4.4. A photo of the experimental setup. Since tin melts in the process, the temperature is monitored by the center thermal couple on a bare copper substrate instead of the actual sample.

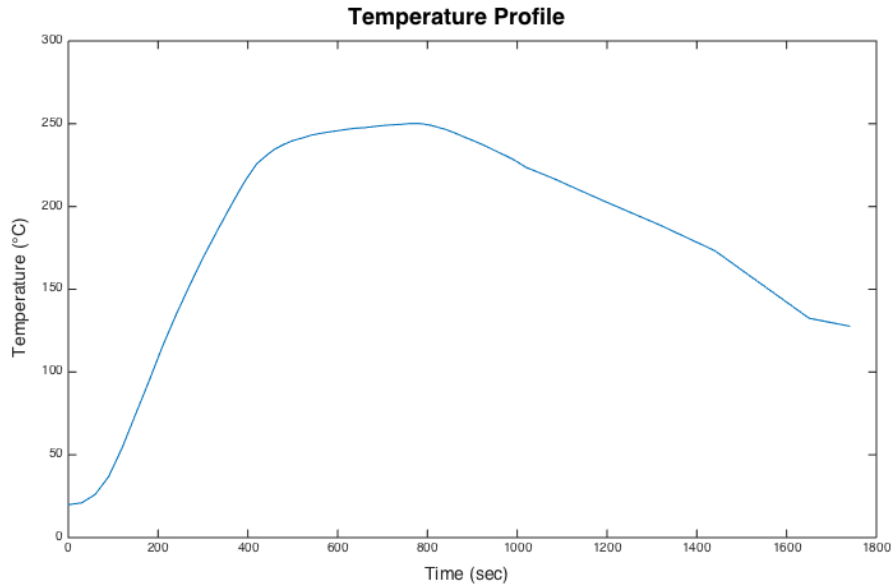


Figure 4.5 Temperature profile of the reflow process in the vacuum bonder.

#### 4.2.2 Results and Discussion

The surface of the samples after reflowing showed some difference. As shown in Figure 4.6, the surface finishes are different for (Ag)In coated Cu and bare Cu samples. Different surface behavior during reflowing process indicates the surface energy and wettability difference. Wetting describes the ability of a liquid in contact with solid surface, where the wettability is observed by the contacting or wetting angle between the surface and liquid. If wetting angle is smaller than  $90^\circ$ , the surface has a relatively high wettability and if the wetting angle is larger than  $90^\circ$ , the wettability is low. Sn on (Ag)In coated Cu was observed to be more spread out compare to that on bare Cu, which indicating the wettability of Sn on (Ag)In coated Cu is better then on bare Cu. High wettability is preferred in this case because the solder can make a better contact with the substrate, and potentially make the solder joint more reliable.



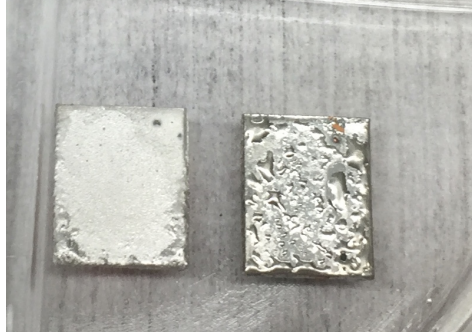


Figure 4.6. As-reflowed Sn soldering reaction samples with (Ag)In coated Cu substrate on the left side and bare Cu substrate on the right side.

Since other samples were aged in a convectional furnace, the surfaces were exposed to air during aging. Aging study is an accelerated way to see how the solder joint performs in long term. The surfaces of the samples after aging are shown in Figure 4.7. For the samples with bare Cu substrate, the surface appears much darker than the ones with (Ag)In coated layer, which is also an indication of (Ag)In coated samples get oxidize much harder than the ones with bare Cu substrate.

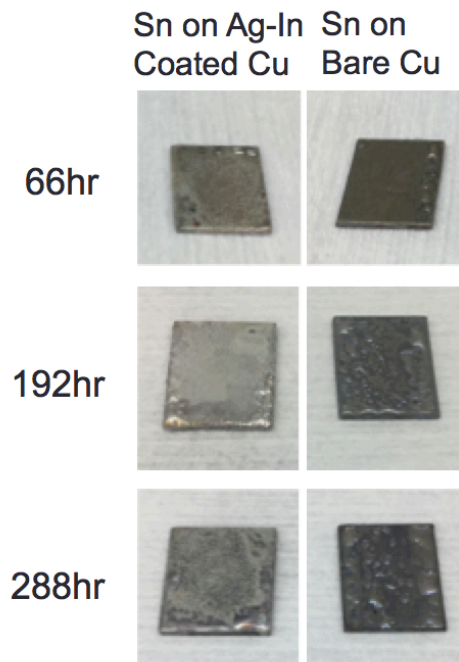


Figure 4.7. Surface of Sn on (Ag)In Coated Cu and Sn on Bare Cu samples after different hours of aging at 175°C.

To observe the intermetallic growth in the soldering reaction, the samples were cut into cross-sections and polished by silicon carbide sand papers and diamond suspension. The cross-sections were etched by diluted HCl and observed under SEM, images of as reflowed samples are shown in Figure 4.8. For bare Cu sample, it is expected that both  $\text{Cu}_6\text{Sn}_5$  and  $\text{Cu}_3\text{Sn}$  IMC would grow at the Cu-Sn interface. At early stage, scallop-shaped  $\text{Cu}_6\text{Sn}_5$  grows with a very thin layer of  $\text{Cu}_3\text{Sn}$  at Cu interface. Figure 4.8(b) shows typical IMC growth of Cu-Sn reflow reaction. On the other hand, (Ag)In coated samples shows a similar appearance under BSE image except some small IMCs grown in the Sn matrix. According to the EDS results, the small particles are  $\text{Ag}_3\text{Sn}$  IMC. The difference of Cu-Sn IMC thickness between (Ag)In coated and bare Cu sample was not obvious at as reflowed stage.

EDX mapping as also been done on the (Ag)In coated sample to examine the element distribution, as shown in Figure 4.9. Note that due to the low indium concentration and EDX resolution limit that discussed in section 3.2, indium mapping is not available. In Sn on (Ag)In coated Cu samples,  $\text{Ag}_3\text{Sn}$  sometimes embedded in scallop-shaped  $\text{Cu}_6\text{Sn}_5$  layer but most of the time scattered in Sn matrix. The IMC growth of Sn and (Ag)In coated Cu behaves similar to using Sn3.5Ag as solder and react with Cu. In the reflow reaction between Sn3.5Ag and Cu, Ag forms  $\text{Ag}_3\text{Sn}$  in the Sn matrix and on top of scallop-shaped  $\text{Cu}_6\text{Sn}_5$  [13].

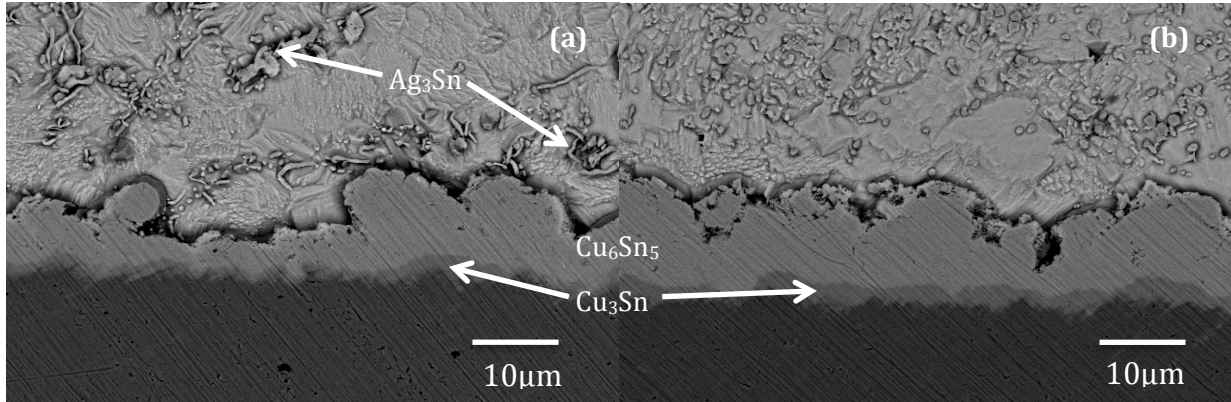


Figure 4.8. Cross-section SEM (BSE mode) image of as reflowed samples of (a) Sn on (Ag)In coated Cu, (b) Sn on bare Cu.

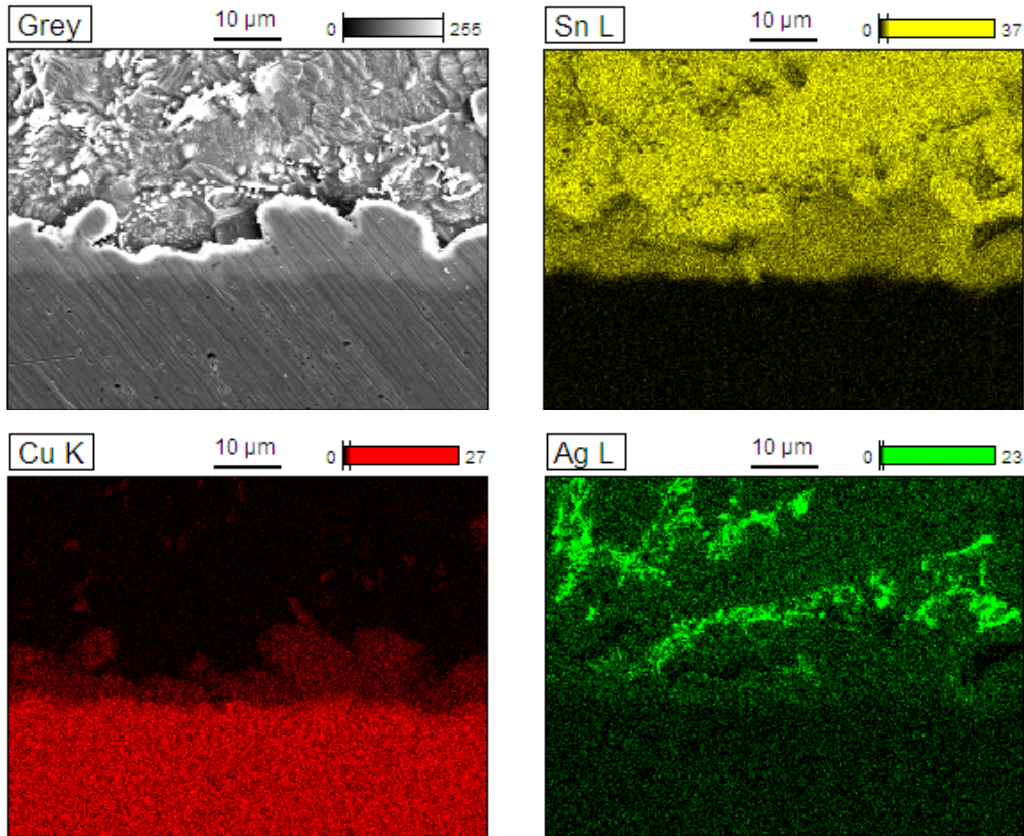


Figure 4.9. EDX mapping of as reflowed Sn on (Ag)In coated Cu sample.

The cross-sections were also prepared for 66hr, 192hr, and 288hr of aging at 175°C. SEM images are shown in Figure 4.10. During aging, there's an obvious difference in  $\text{Cu}_3\text{Sn}$  layer thickness between (Ag)In coated sample and the bare Cu substrate sample.  $\text{Cu}_6\text{Sn}_5$  in both samples are similar in thickness, yet  $\text{Cu}_3\text{Sn}$  layer is much thicker in Sn on bare Cu than in Sn on (Ag)In coated Cu sample. To make a clearer comparison, the thicknesses of different IMC layers are plotted in Figure 4.11. From the plot, several things can be observed:  $\text{Cu}_6\text{Sn}_5$  grows faster in bare Cu sample;  $\text{Cu}_3\text{Sn}$  shows an obvious gradual increase in thickness during aging in both (Ag)In coated and bare Cu sample; both  $\text{Cu}_6\text{Sn}_5$  and  $\text{Cu}_3\text{Sn}$  layer were significantly thinner in (Ag)In coated sample than in bare Cu sample after aging.

Because both  $\text{Cu}_6\text{Sn}_5$  and  $\text{Cu}_3\text{Sn}$  are brittle IMCs, having a thinner layer can reduce the chance of breaking the joints at IMC phase and increase the joint reliability.

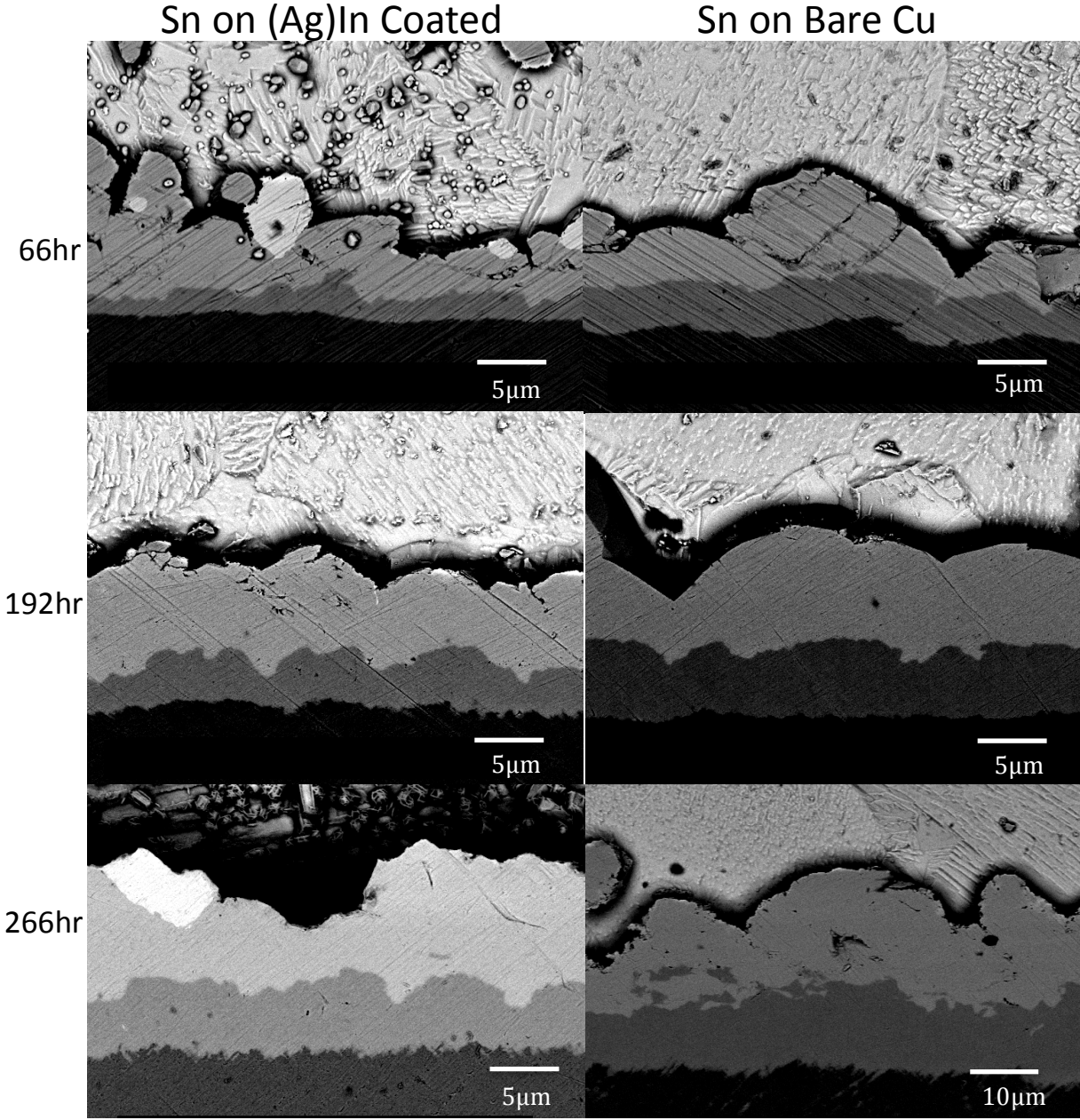


Figure 4.10. Cross-section SEM (BSE) image of Sn on (Ag)In coated Cu and Sn on bare Cu samples aged at 175°C for different hours.

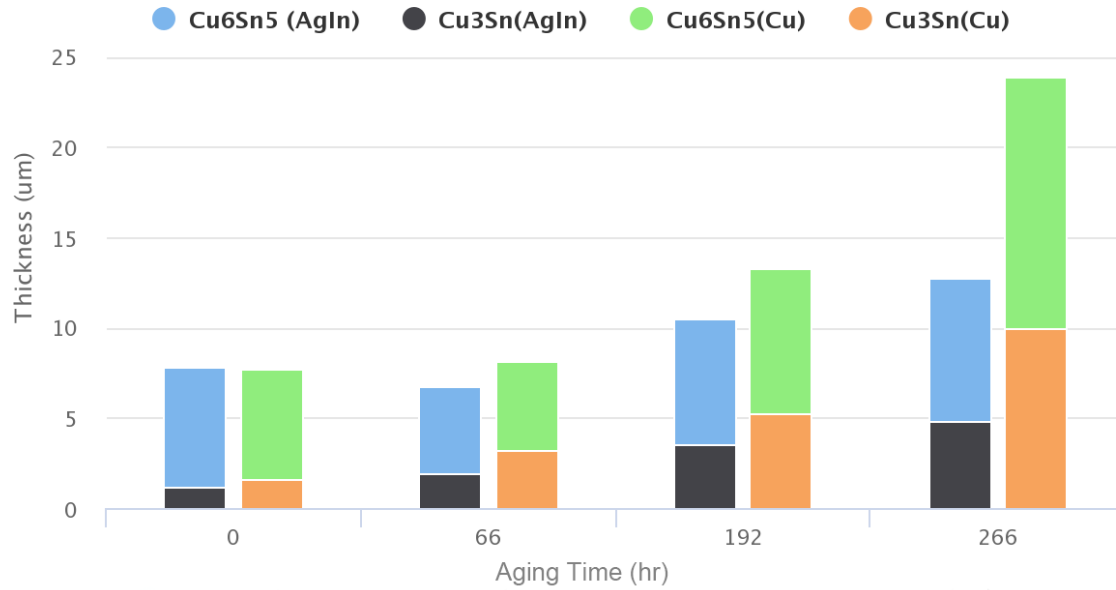


Figure 4.11. Plot of  $\text{Cu}_6\text{Sn}_5$  and  $\text{Cu}_3\text{Sn}$  IMC thicknesses (both separated and combined) of (Ag)In coated and bare Cu samples at different aging time.

According to the observed cross-sections for different aging time, an illustration of IMC growth in Sn on (Ag)In coated Cu sample has been shown in Figure 4.12. During reflow, Sn melts and (Ag)In layer firstly dissolved into Sn matrix and starts to form  $\text{Ag}_3\text{Sn}$  IMC, In remains in solid solution form. Sn meets Cu and starts to form and grow scallop-shaped  $\text{Cu}_6\text{Sn}_5$ . According to the previous study [14], a very thin layer of  $\text{Cu}_3\text{Sn}$  is also grown at the interface at early stage of the reaction. Dissolving of (Ag)In, forming  $\text{Ag}_3\text{Sn}$  and growth of  $\text{Cu}_6\text{Sn}_5$  are likely to happen at the same time because some  $\text{Ag}_3\text{Sn}$  are embedded in the  $\text{Cu}_6\text{Sn}_5$ . During aging, both  $\text{Cu}_6\text{Sn}_5$  and  $\text{Cu}_3\text{Sn}$  gradually grow thicker. Due to the limit amount of (Ag)In in the Sn matrix, no direct observation shows the  $\text{Ag}_3\text{Sn}$  IMC growth during aging.

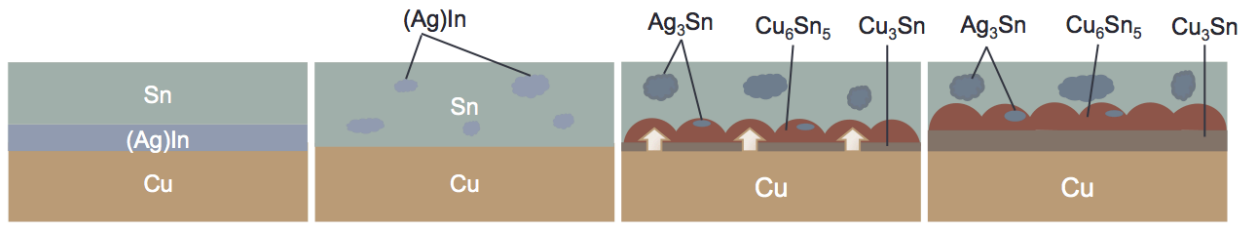


Figure 4.12. An illustration of IMC growth of the reaction between (Ag)In coated Cu and Sn.

## 5. SUMMARY AND CONCLUSIONS

In this study, the possibility of using (Ag)In on Cu substrate as passivation has been investigated. Firstly, the reaction study has been done on bulk (Ag)9.5In disk and Sn and the reacted samples were characterized by SEM, EDX and XRD. The result shows that (Ag)In-Sn reaction behaves very similar to Ag-Sn reaction; In doesn't form any additional IMC, and it rather stays as solid solution phase in the reaction. Secondly, aging study of (Ag)In coated Cu shows significantly less oxidation occurred at surface compare to that of bare Cu, showing that using (Ag)In coating as protection layer can extend the storage life of Cu leadframes in the industry. Lastly, soldering reaction between Sn and (Ag)In coated Cu shows that the substrate remains solderability with the protective coating. Moreover, compare to the soldering reaction with bare Cu, coated sample has a better wettability and much thinner IMC layer growing at interface, especially after aging at 175°C. The existence of coating layer suppresses the growing of IMC between solder and leadframe and improves the joint reliability especially in long-term usage. The whole process didn't use any lead-containing material or flux. The research shows that (Ag)In is a promising environmental friendly and economical passivation alternative on copper leadframes and potentially other packaging uses.



## REFERENCE

- [1] K.N. Tu , Solder Joint Technology, *Springer*, 2007.
- [2] K.N. Tu, J.C.M. Li, Spontaneous Whisker Growth on Lead-free Solder Finishes, *Materials Science and Engineering A*, 2005, 409: 131–139.
- [3] D.C. Abbott, R.M. Brook, N. McLelland, J.S. Wiley, Palladium as a Lead Finish for Surface Mount Integrated Circuit Packages. *IEEE Transactions on Components Hybrids and Manufacturing Technology*, September 1991, Vol. 14, No.3: 567-572
- [4] Y. Huo, S.W. Fu, Y.L. Chen, C.C. Lee, A reaction study of sulfur vapor with silver and silver–indium solid solution as a tarnishing test method. *J. Mater. Sci. Mater. Electron.*, 2016 27: 10382–10392
- [5] Y.C. Chan, A.C.K. So, J.K.L. Lai, Growth kinetic studies of Cu–Sn intermetallic compound and its effect on shear strength of LCCC SMT solder joints. *Mater. Sci. Eng., B*, 1998, 55: 5-13
- [6] S.W. Fu, C.Y. Yu, T.K. Lee, K.C. Liu, J.G. Duh, Impact crack propagation through the dual-phased (Cu,Ni)<sub>6</sub>Sn<sub>5</sub> layer in Sn–Ag–Cu/Ni solder joints. *Mater. Lett.*, 2012, 80: 103-105
- [7] O.A. Ogunseitan, Public health and environmental benefits of adopting lead-free solders. *JOM*, 2007, 59: 12.
- [8] Scanning Electron Microscope A to Z. JEOL.  
[https://www.jeol.co.jp/en/applications/pdf/sm/sem\\_atoz\\_all.pdf](https://www.jeol.co.jp/en/applications/pdf/sm/sem_atoz_all.pdf)
- [9] ISAAC: Imaging Spectroscopy and Analysis Centre, *University of Glasgow*,  
<https://www.gla.ac.uk/schools/ges/researchandimpact/researchfacilities/isaac/services/scanningelectronmicroscopy/>
- [10] X-ray Diffraction. *Rigaku*, <https://www.rigaku.com/en/techniques/xrd>

- [11] Electron Beam Evaporation: Overview. *Angstrom Engineering*.  
<https://angstromengineering.com/tech/electron-beam-evaporation/>
- [12] G.P. Vassilev, E.S. Dobrev, J.C. Tedenac, Experimental study of the Ag-Sn-In phase diagram. *J. Alloys Compd.* 2005, 399: 118-125
- [13] T.L. Su, L.C. Tsao, S.Y. Yang, T.H. Chuang, Morphology and Growth Kinetics of Ag<sub>3</sub>Sn During Soldering Reaction Between Liquid Sn and an Ag Substrate. *JMEPEG*, 2002, 11: 365-368
- [14] J.F. Li, P.A. Agyakwa, C.M. Johnson, Interfacial reaction in Cu/Sn/Cu system during the transient liquid phase soldering process. *Acta Materialia* 2011, 59: 1198–1211
- [15] J. Yoon, B. Noh, B. Kim, C. Shur, S. Jung, Wettability and interfacial reactions of Sn–Ag–Cu/Cu and Sn–Ag–Ni/Cu solder joints. *J. Alloys Compd.* 2009, 486: 142–147